



Total Control

Advanced integrated supervisory and wind turbine control for optimal operation of large Wind Power Plants

Title (of deliverable): Dynamic wake induction control

Deliverable no.: 4.5

Delivery date: (17.5.2022)

Lead beneficiary: KUL

Dissemination level: Public



This project has received funding from the European Union's Horizon 2020 Research and Innovation Programme under grant agreement No. 727680

Author(s) information (alphabetical):

Name	Organisation	Email
Ishaan Sood	KU Leuven	Ishaan.sood@kuleuven.be
Johan Meyers	KU Leuven	Johan.meyers@kuleuven.be

Document information

Version	Date	Description	Prepared by	Reviewed by	Approved by
1	02.02.2022		Ishaan Sood		
2	19.02.2022			Johan Meyers	
3	29.03.2022				Karl Menz

TABLE OF CONTENTS

Table of Contents	3
1. Executive Summary.....	4
2. Introduction	5
3. Description of Dynamic Induction Control Approach.....	6
3.1 Background.....	6
3.2 Controller for dynamic signal tracking	7
4. Reference database and selected cases	11
5. Results	13
5.1 Controller Performance.....	13
5.2 Wake recovery	14
5.3 Power Production	15
5.4 Turbine Fatigue.....	16
6. Conclusions	18
7. Bibliography.....	19

1. EXECUTIVE SUMMARY

One of the core activities of the TotalControl project is the study and development of advanced coordinated wind farm control algorithms to improve overall performance. An effective way of increasing energy extraction in a wind farm is by changing the static yaw set-points depending on the mean wind direction. An alternative approach is dynamic induction control, which involves dynamically changing turbine power and thrust set-points with time scales in the range of 20 to 30 seconds. The strategy has been shown to facilitate wake breakdown, thus leading to faster wake recovery and improved power production. While research was recently conducted on optimal dynamic induction control for determining turbine setpoints which promote this wake recovery, the studies however were either restricted to simplistic representation of turbine physics, or limited to a two turbine setup due to the expensive computational requirements for blade resolved studies. Furthermore, it was also observed that the enhanced wake recovery due to dynamic control was obtained only when controlling the upstream turbines, and the effect could not be reliably replicated deeper within large wind farm arrays.

Therefore, this report aims to conduct a feasibility study of dynamic induction control in large wind farms by implementing a simple control strategy which imposes sinusoidal thrust variation of the upstream turbines within a farm to promote wake recovery. The study also aims to investigate the practicality of dynamically varying turbine setpoints by investigating the effect of such a strategy on the increase of fatigue in turbine components. Simulations are conducted using large eddy simulations, with turbines represented in the domain using aeroelastic models. A reference wind farm database which was previously developed within the total control project was used as a benchmark against which the merits and demerits of the dynamic induction control strategy could be evaluated.

2. INTRODUCTION

In order to benefit from economies of scale and facilitate ease of installation and maintenance, wind turbines are often installed together in clusters called wind farms. However, aerodynamic coupling between upstream and downstream turbines due to wake overlap within a farm can lead to significant operational losses in power production. This occurs due to the focus of conventional controllers on individual turbine level greedy control, while the farm level interactions are generally ignored. Recent research has shown that through coordinated farm control strategies such as axial induction control, an enhanced energy extraction up to 20% could be achieved for the entire farm [1], [2]. This work aims to investigate a Dynamic Axial Induction Control (DAIC) strategy, which involves varying the operational set-point of the upstream turbines within a wind farm to facilitate wake mixing and breakdown, hence boost power production of downstream turbines [3].

A first consequence of axial induction control is that the first-row turbines may produce less power compared to a scenario where only conventional controllers are used. However, on a farm level, this decrease in power production from the upstream turbines could be compensated by a gain in efficiency of the downstream turbines. A second consequence is that axial induction control may affect the structural loading of the turbine, as unsteady loading due to varying thrust forces could lead to increased structural fatigue. An increase in fatigue would limit the lifetime of the turbine and lead to possibly higher maintenance costs. Therefore, it is essential to study the effect of tracking dynamic signals on both the farm power production as well as on the lifetime reduction of the turbines.

Therefore, the current document outlines a feasibility study conducted for the DAIC strategy, by evaluating its merits and demerits when compared to conventional wind turbine control. The study utilizes the TotalControl reference wind farm database as the benchmark, which was a database consisting of the TotalControl Reference Wind Power Plant (TC RWP) operating under different atmospheric conditions while using conventional wind turbine control. Comparisons are made on the basis of power gains, fatigue degradation and wake mixing within the farm to determine the influence of DAIC on farm performance.

This document is outlined as follows. First, a brief overview is provided about the previous work carried out in the development of the DAIC strategy, and the details of the controller modifications required to implement is presented in Section 3. Information of the wind farm reference database, details of the Large Eddy Simulation (LES) suite used to conduct the experiments and specifications of the cases selected for evaluating the performance of DAIC are outlined in Section 4. Section 5 presents the results of the simulations and an evaluation of farm performance when compared with the reference benchmark cases. Finally, Section 6 provides the conclusions of the study.

3. DESCRIPTION OF DYNAMIC INDUCTION CONTROL APPROACH

3.1 BACKGROUND

In a novel approach, Goit & Meyers investigated dynamic axial induction control by using wind turbines as dynamic flow devices acting upon the turbulent ABL flow [1]. Through adjoint based optimization to determine the dynamic set points, the turbines are able to engage in active symbiosis with the physics governing the turbulent flow to increase overall power extraction, and energy extraction was increased by 16% for of a fully-developed very large wind farm. Instead of resolving the effects of tip speed ratio and blade pitch angle on the induced thrust force, they perform optimal axial induction control by dynamically controlling individual turbine thrust coefficients directly. Munters & Meyers further extended this work and presented a simple sinusoidal thrust control approach that successfully mimics this process with a robust increase in power extraction in the second row [3]. The aim of their work was to mimic the quasi-periodic shedding of vortex rings which lead to enhanced wake recovery, as seen in Figure 1, through the use of simple periodic variations in the thrust coefficient.

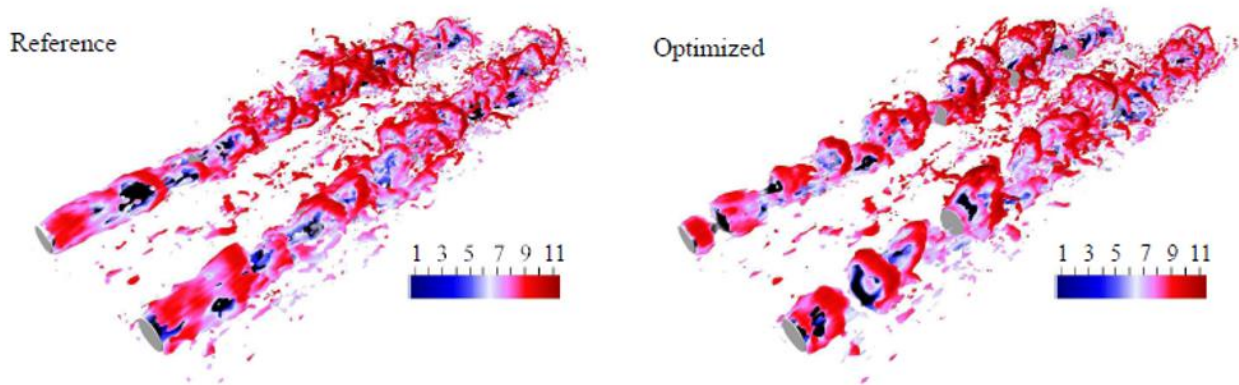


FIGURE 1 INSTANTANEOUS ISOSURFACE OF VORTICITY MAGNITUDE OF WIND-FARM FLOW FIELD FOR THE REFERENCE (LEFT) AND OPTIMIZED (RIGHT) CASE. FIGURE TAKEN FROM [3]

To this end, the Betz-optimal disc based thrust coefficient $C_T' = 2$ is perturbed by a sinusoidal signal, parametrized by its amplitude A , and a non-dimensional frequency in the form of the Strouhal number $St = fD/U_\infty$ through the expression

$$C_T'(t) = 2 + A \sin\left(2\pi St \frac{tU_\infty}{D}\right)$$

In contrast to the normal thrust coefficient C_T , the disc based thrust coefficient C_T' is evaluated based on the velocity measured at the disc instead of the free-stream velocity, as the free stream velocity is usually difficult to determine in a wind farm environment [1]. By conducting a parameter sweep on the parameters A and St in a number of wind farm Large Eddy Simulations (LES), Munters and Meyers determined that a maximal power increase of about 5% could be achieved using the combination $(St, A) = (0.25, 1.5)$. However, it was determined that the technical feasibility of obtaining the extreme C_T' of 3.5 could only be possible by altering the chord length of the turbine blades by up to 50%, or by using extreme turbine pitch and rotational speed combinations. Furthermore, it was determined that the positive effect of this approach

was only evident if DAIC was applied to the first row of turbines, and no significant benefit was observed if applied to turbines deeper within the farm. Additionally, all the simulations were carried out by using the Actuator Disc Model (ADM), which is a simplistic representation of wind turbines in the LES domain and neglects the effects of blade resolved effects and rotor rotation. While Yilmaz and Meyers did explore the use of the blade resolved Actuator Line Model (ALM) to determine optimal dynamic induction setpoints for a pair of inline turbines, the study was restricted to the use of uniform inflow and could not be extended to large wind farms due to the very fine spatio-temporal requirements of ALM [4].

The current work aims to investigate these shortcomings by first developing a controller which can dynamically track realistic thrust coefficient set points, and then simulate its operation in wind farm environment through the use of LES. The dynamic control strategy chosen for investigation is the one developed by Munters & Meyers, due to the simplicity of its implementation. Turbines in the LES domain are parametrized using the Aeroelastic Actuator Sector Model (AASM). The AASM allows for a more accurate wind turbine representation compared to the ADM which was used in the previously mentioned studies on DAIC, while allowing for a coarser grid resolution than the ALM, thus enabling the study of large wind farms [5]. Additionally, use of an aeroelastic implementation would allow to evaluate the effect of tracking such dynamic thrust setpoints on the turbine fatigue, which was not investigated in previous studies.

3.2 CONTROLLER FOR DYNAMIC SIGNAL TRACKING

Based on the function of the conventional wind turbine, three main regions can be distinguished in the wind turbine operation curve, as can be seen in Figure 2. For wind speeds below the cut-in wind speed, the wind turbine is parked and no power is produced and is said to be operating in Region 1. For wind speeds between the cut-in speed and the rated speed, the wind turbine tries to extract the maximum power, P_{rated} , from the wind. This action is called Maximum Power Point Tracking (further abbreviated MPPT) and occurs in Region 2. Above rated wind speed, the wind turbine limits its power production by pitching the blades. This action prevents that the nominal power is exceeded and characterises Region 3. A fourth Region includes the shut-down procedure of the wind turbine in case of winds above the cut-out speed. The current work, as previous DAIC studies, focuses on wind speeds associated with Region 2 operation throughout the farm. From a wind-farm power maximization perspective, these speeds are relevant for coordinated wind-farm control since for turbines operating below rated power, more favourable local flow conditions directly translate into increased power extraction.

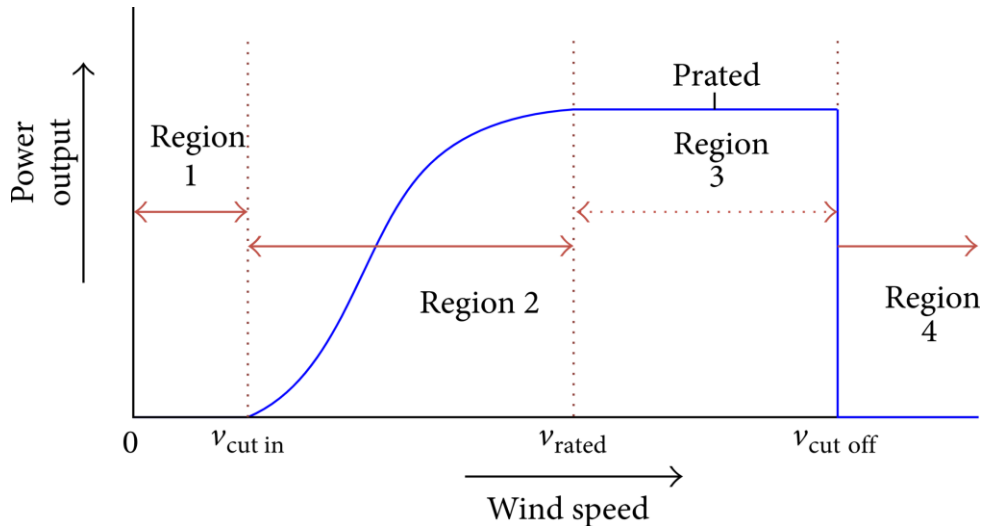


FIGURE 2 DIFFERENT OPERATION STATES OF A CONVENTIONAL WIND TURBINE [6].

The turbine and controller of focus in this document will be the DTU 10 MW turbine [7], which is a reference wind turbine that has been extensively used in the TotalControl project for developing coordinated farm control strategies. The desired aerodynamic performance of a turbine and disc based thrust coefficient C_T' for dynamic setpoint tracking can be achieved using different combinations of turbine tip speed ratio λ or turbine pitch β , as can be seen by the performance surface of the DTU 10MW turbine in Figure 3. For simplicity, in the current work we restrict ourselves to only variation in tip speed ratio in Region 2 operation, and the turbine pitch is kept at 0, which is the ideal value for Region 2.

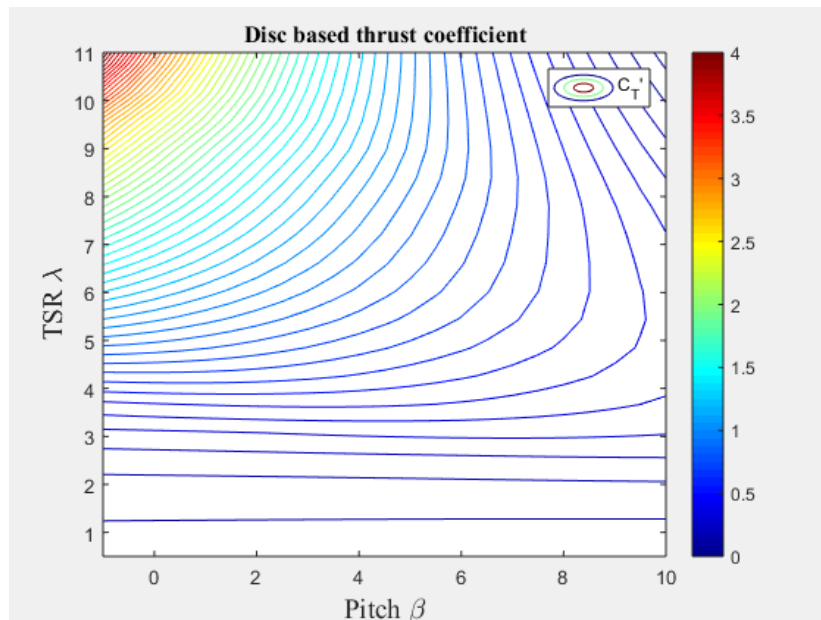


FIGURE 3 PITCH AND TSR COMBINATIONS FOR ACHIEVING DIFFERENT THRUST COEFFICIENT VALUES FOR THE DTU 10MW TURBINE. FIGURE OBTAINED BY ANALYZING THE DTU 10MW TURBINE IN THE SOFTWARE AERODYN [8].

Different kinds of controllers could meet the present requirements of tracking a dynamic reference signal. PID-controllers, however, offer a good compromise between simplicity of design and performance. Furthermore, PID-controllers are the most widespread industrial controllers,

and are already actively used for wind turbine control. For this reason, a PID-controller is designed in this work using pole placement, which relies on the error of tracking a reference thrust coefficient for determining the generator torque and hence rotor speed. To design the controller for tracking a reference dynamic thrust coefficient, the drive train of a wind turbine can be represented by a simple model shown in Figure 4 comprising of a stiff shaft with inertia J , rotating with a speed ω_r , with aerodynamic torque T_{aero} acting on one end, and generator torque T_{gen} acting on the other end.

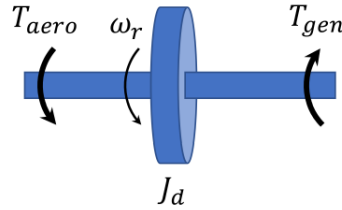


FIGURE 4 SIMPLE REPRESENTATION OF A WIND TURBINE OPERATION

Thus, the non-linear drive train equation for a wind turbine can be written as

$$J\dot{\omega} = T_{aero}(\lambda, \beta) - T_g,$$

where $\lambda = \omega R/v$ is the tip-speed ratio, R is the turbine radius, and v is the turbine inflow velocity. A general PI controller from disc-based thrust coefficient error for generator torque controller can thus be defined as

$$\Delta T_g = k_p(C'_T - C'_{T_r}) + k_I \int (C'_T - C'_{T_r})dt$$

Where k_p is the proportional gain, k_I is the integral gain C'_T is the previous thrust coefficient value and C'_{T_r} is the thrust coefficient value to be tracked. Defining ϕ as the error between the tracking and reference signals, the following definitions can be made, and assuming that for a small dt the C'_{T_r} remains quasistatic,

$$\begin{aligned} \dot{\phi} &= C'_T - C'_{T_r} \\ \ddot{\phi} &= \dot{C}'_T \end{aligned}$$

T_{aero} and T_g can thus be linearized about the tracking point (with the assumption of zero pitch angle), and combining all the equations above leads to a linear closed loop equation for a small perturbation about $C'_T = \phi + C'_{T_r}$ as follows

$$J \left(\frac{v}{R} \frac{\partial \lambda}{\partial C'_T} \right) \ddot{\phi} + \left(k_p - \frac{\partial T_{aero}}{\partial C'_T} \right) \dot{\phi} + k_I \phi = 0.$$

The above equation can be combined with a standard second order system of the form

$$s^2 + 2\zeta\omega_n s + \omega_n^2 = 0,$$

with ζ the damping ratio, and ω_n the system's natural frequency. Thus by comparing coefficients, we can obtain the values of the proportional and integral gains of the PI system as follows

$$k_p = 2J\zeta\omega_n \frac{v}{R} \frac{\partial \lambda}{\partial C_T'} + \frac{\partial T_{aero}}{\partial C_T'},$$

$$k_i = \omega_n^2 J \frac{v}{R} \frac{\partial \lambda}{\partial C_T'}.$$

Therefore, the PI controller can be tuned by selecting the values of ζ and ω_n which result in the best performance. A common value for the damping ratio ζ is 0.7 and results from a compromise between a small overshoot and a short settling time. A high overshoot would increase the structural loading of the wind turbine, whereas a longer settling time would decrease the performance of the controller in terms of perturbation rejection and reference tracking. Thus, as a rule of thumb, ζ is set to 0.7.

ω_n on the contrary should be chosen carefully such that the non-linear terms that have been neglected in the simplified wind turbine model remain small enough compared to the linear terms. In other words, if ω_n is too high, the non-linear behaviour of the system will gain the upper hand and be a source of instability for the controlled system. In the present case, the period of vibration in the shaft of the DTU 10 MW RWT is 0.54 seconds as per the turbines specifications. A second rule of thumb consists of taking one order of magnitude higher for the period of ω_n , which gives a period (rounded) of 5 seconds. Thereby, $\omega_n = 2\pi / 5$ rad/s.

The developed controller is tested on the SP-Wind LES platform, by tracking a dynamic thrust coefficient signal with amplitude 0.2 and frequency 50s. The controller was tested for a single DTU 10MW turbine operating under uniform inflow velocity of 8 m/s. From Figure 5, it can be seen that the controller performs very well and is able to track the dynamic signal successfully.

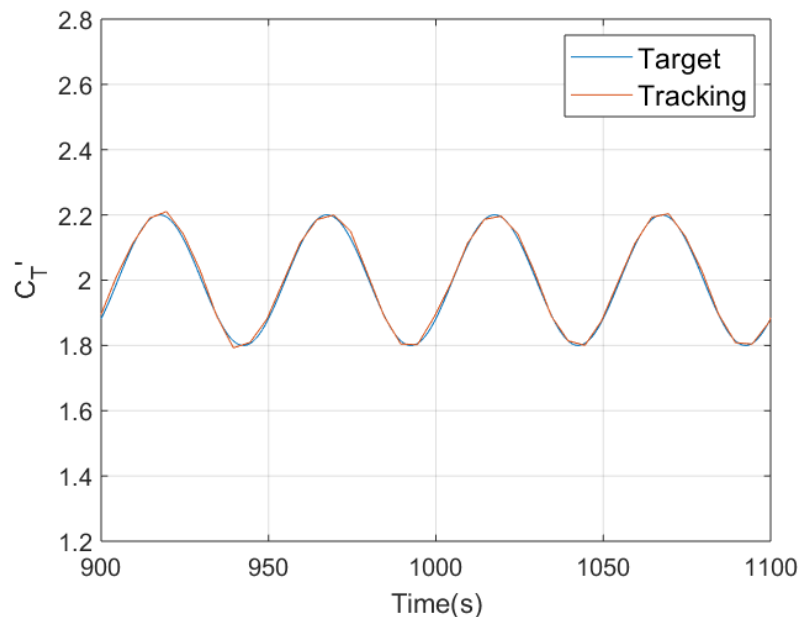


FIGURE 5 SIGNAL TRACKING RESULTS FOR TESTING THE DEVELOPED CONTROLLER.

4. REFERENCE DATABASE AND SELECTED CASES

Reference windfarm cases operating under normal operation are required to analyze the effects of dynamic induction control on farm performance. To this end, we make use of the publicly available TotalControl reference windfarm database which comprises of numerical measurements using high fidelity LES spanning different atmospheric conditions and wind directions for the TotalControl reference windfarm [9]. The TotalControl Reference Wind Power Plant (TC RWP) is a virtual setup which comprises of 32 DTU 10 MW turbines, separated by 5D spacing in the vertical and horizontal directions. The layout of the TC RWP is presented in Figure 6. Two different normal operation cases with different wind directions but the same inflow are chosen from the reference database for this study. Both the cases have the same inflow, a Pressure Driven Boundary Layer (PDBL) with base wall roughness of 2×10^{-4} , which is a simplistic representation of the atmospheric boundary layer. Different wind directions are obtained by rotating the entire wind farm in the simulation domain, hence obtaining a different configuration of staggered and aligned wind turbines, as shown in Figure 7. It can be seen that in the first configuration with a wind direction of 270° , the spacing between the aligned turbines is 10 rotor diameters, or 10D, while in the second configuration with a wind direction of 0° , the turbine spacing is only 5D. Hence the two configurations allow us to study the effect of DAIC while considering the impact of wind direction and turbine spacing.

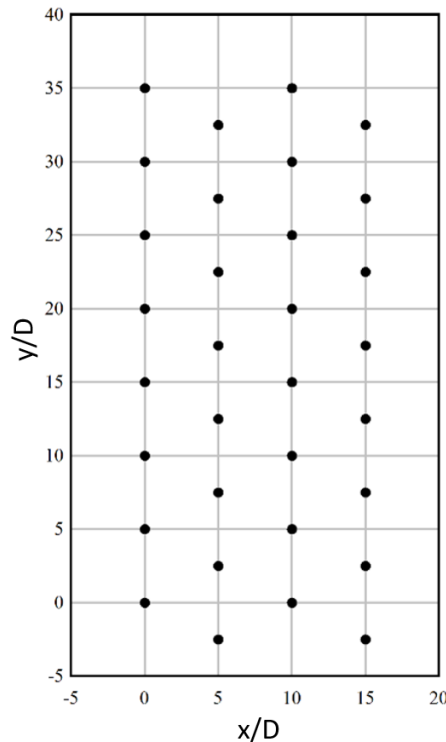


FIGURE 6 PLANVIEW OF TCRWP LAYOUT COMPRISING OF 32 DTU 10 MW TURBINES. TURBINES ARE NUMBERED 1 TO 32 BOTTOM TO TOP AND LEFT TO RIGHT.

For DAIC, as detailed in the previous section, the main parameters are the amplitude of the disc based thrust coefficient, the frequency of the sine wave, and the turbine controlled. As previous research has shown that the highest benefit from DAIC is obtained when only the first turbine in an array is controlled dynamically, we will restrict our analysis to applying the strategy to only one upstream turbine in each case and then evaluating its effect on farm performance. Two different combinations of amplitude and Strouhal number are considered to study the effect of changing these parameters in combination with turbine spacing. All the selected cases have been summarized in Table 1. The reasoning behind selecting the combination of amplitude and Strouhal number is explained in Section 5.1.

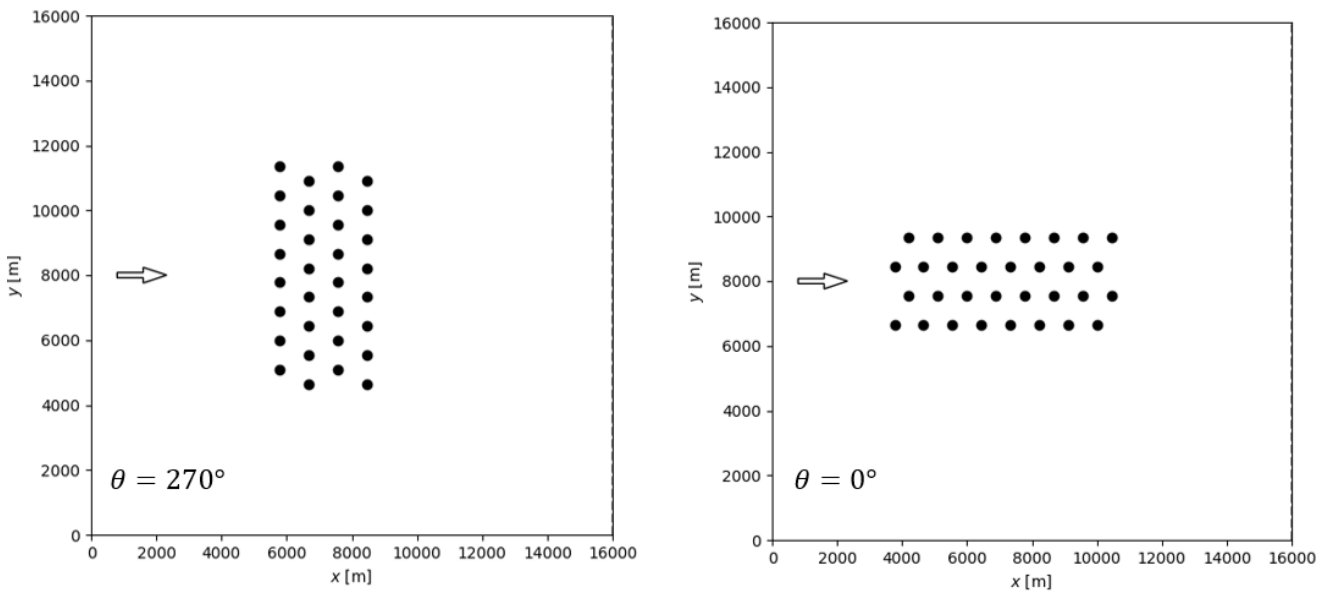


FIGURE 7 ORIENTATION OF THE WIND TURBINES FOR THE 2 STUDIED CONFIGURATIONS. LEFT FIGURE HAS A WIND DIRECTION OF 270 DEGREES, WHILE THE FIGURE ON THE RIGHT HAS A WIND DIRECTION OF 0 DEGREES.

Similar to the reference wind farm database, all the simulations are carried out in a Large Eddy Simulation (LES) environment using the code SP-Wind [1], [2], [10]. Spatial discretization in SP-Wind is performed by combining pseudo-spectral schemes with fourth-order energy-conservative finite differences. The equations are marched in time using a fully explicit fourth-order Runge-Kutta scheme, and grid partitioning is achieved through a scalable pencil decomposition approach. Subgrid-scale stresses are modeled with a standard Smagorinsky model with wall damping. Wind turbines are modeled by an actuator sector model, coupled with a nonlinear flexible multi-body dynamics model [5]. Turbulent inflow conditions for wind-farm simulations are generated in separate precursor simulations [11]. A streamwise slab of the velocity and temperature field is stored to disk when running the precursor, and is later introduced in the wind-farm domain by means of body forces in a so-called fringe region. Similar to the reference database, the simulations are divided into 2 parts. First, a spin-up period of 15 min is initiated for the settling of start-up transients, followed by 60 minutes of data collection. The LES time step is set to 0.5s, while the structural solver operates at a higher frequency of 100 Hz. The general domain parameters for the LES simulations are outline in Table 1.

TABLE 1 SPECIFICATIONS OF SIMULATED CASES

Case No.	Wind direction (degrees)	Amplitude	Strouhal number	Controlled turbine
1	270	0.3	0.25	1
2	270	0.6	0.125	1
3	0	0.3	0.25	8
4	0	0.6	0.125	8

TABLE 2 SIMULATION PARAMETERS FOR SP-WIND

	Variable	Values
Domain size	$L_x \times L_y \times L_z$	$16 \times 16 \times 1.5 \text{ km}^3$
Grid	$N_x \times N_y \times N_z$	$1200 \times 1200 \times 225$
Resolution	$\Delta_x \times \Delta_y \times \Delta_z$	$13.33 \times 13.33 \times 6.66 \text{ m}^3$
Spinup time	T_{spin}	15 min
Simulation time	T	60 min
Time steps	$\Delta t_{LES}, \Delta t_{struct}$	0.5 s, 0.01 s

5. RESULTS

In this section, the influence of DAIC on farm performance is evaluated by comparing the results from the selected cases against the reference wind farm database results.

5.1 CONTROLLER PERFORMANCE

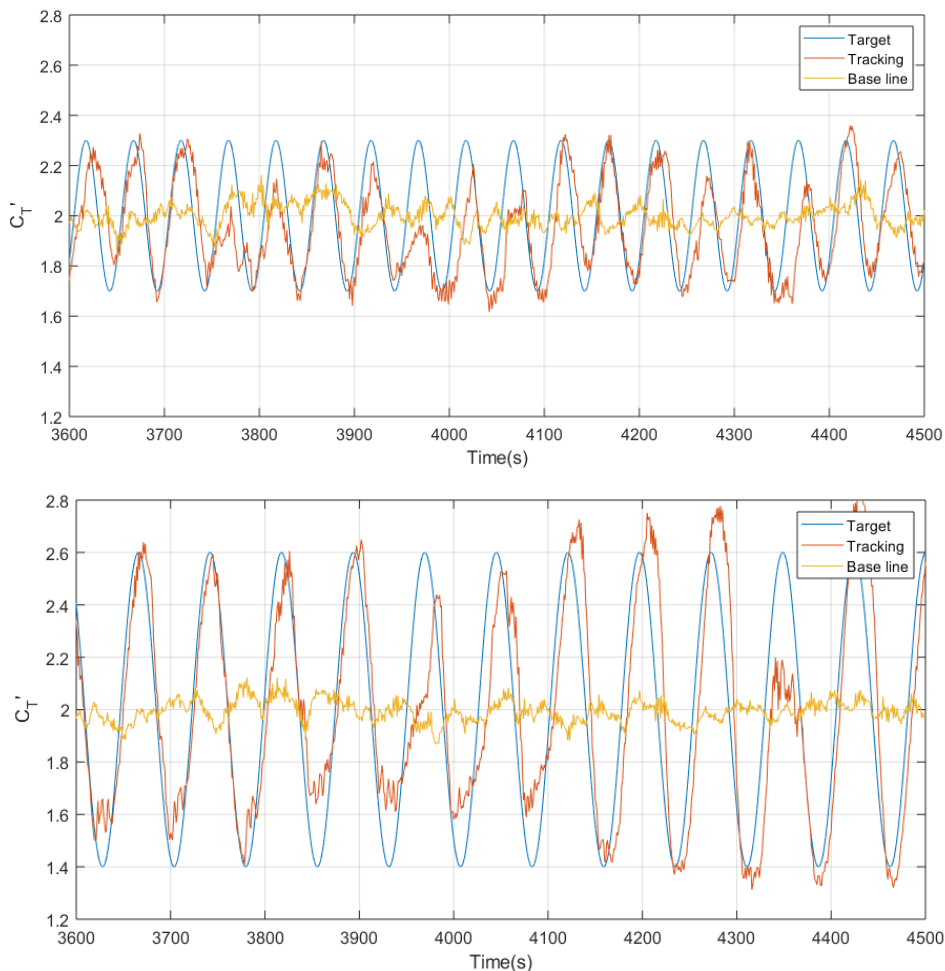


FIGURE 8 CONTROLLER PERFORMANCE FOR TRACKING THE 2 SINE SIGNALS. TOP FIGURE RELATES TO CASES 1 & 3, BOTTOM FIGURE TO CASES 2 & 4. THE YELLOW LINE SHOWS THE THRUST COEFFICIENT OF A CONTROLLER EMPLOYING MPPT.

While the controller designed in 3.2 was shown to work well for uniform inflow, it is essential to analyze how the controller performs when the turbine is subjected to a turbulent inflow velocity field. From Figure 8, it can be seen that the controller performs better for a case with a lower Strouhal number of 0.125, hence slower variation of the thrust signal, compared to a signal with the optimal Strouhal number of 0.25 as determined by Munters & Meyers. The lower Strouhal number however allows us to achieve reasonable tracking of a dynamic thrust coefficient with a higher amplitude of 0.6, which would lead to enhanced wake recovery as per the same study [3]. A higher thrust coefficient value would violate the rotor speed restrictions of the turbine, and were hence avoided. It can also be seen that compared to tracking under a uniform inflow, the controllers perform worse when subjected to a turbulent inflow. This is expected due to the added complexity of a varying inflow velocity field, and the large inertia of the turbine rotor. The performance of the controller could be further improved by further tuning or using advanced controllers which are able to account for this disturbance, however for our purposes the current tracking quality is sufficient.

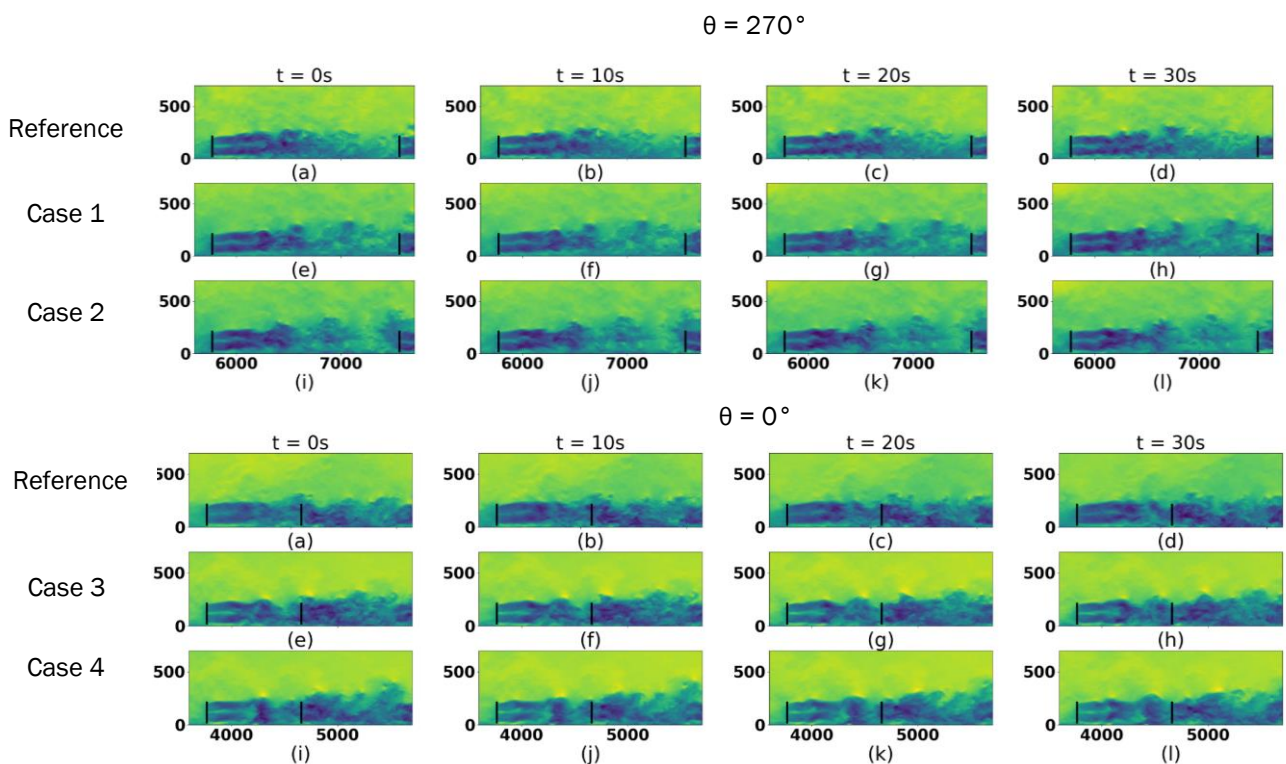


FIGURE 9 INFLUENCE OF TRACKING A DYNAMIC THRUST SIGNAL ON INSTANTANEOUS VELOCITY FIELD.

5.2 WAKE RECOVERY

The influence of tracking a dynamic thrust coefficient setpoint on the wake recovery within the farm can be seen in Figure 9. For cases 1 and 2, the figures show the upstream dynamically controlled turbine (WT 1) and the downstream turbine (WT 17) with a spacing of 10D between them. For cases 3 and 4, the upstream dynamically controlled turbine (WT 8) and downstream turbine (WT 7) are separated by a distance of 5D. Comparisons are made for all the cases with velocity fields from the reference wind farm database with normal operation. In all the cases, it can be seen that the wakes downstream of the controlled turbine break down faster when compared to the reference case, and the effect is greater for cases 2 and 4 with the higher

amplitude of 0.6. However, it can also be observed that the influence on wake recovery decreases with an increase in downstream distance. This can further be verified from Figure 10, where the time averaged wake recovery downstream from the controlled turbine is compared against the reference cases. While the wake recovery is higher than the reference case until a downstream distance of $4.5D$, the benefit is limited for a larger downstream distance of $10D$. Therefore, cases 3 and 4 with a wind direction of 0 and turbine spacing of $5D$ experiences a larger benefit from DAIC than cases 1 and 2 with spacing of $10D$.

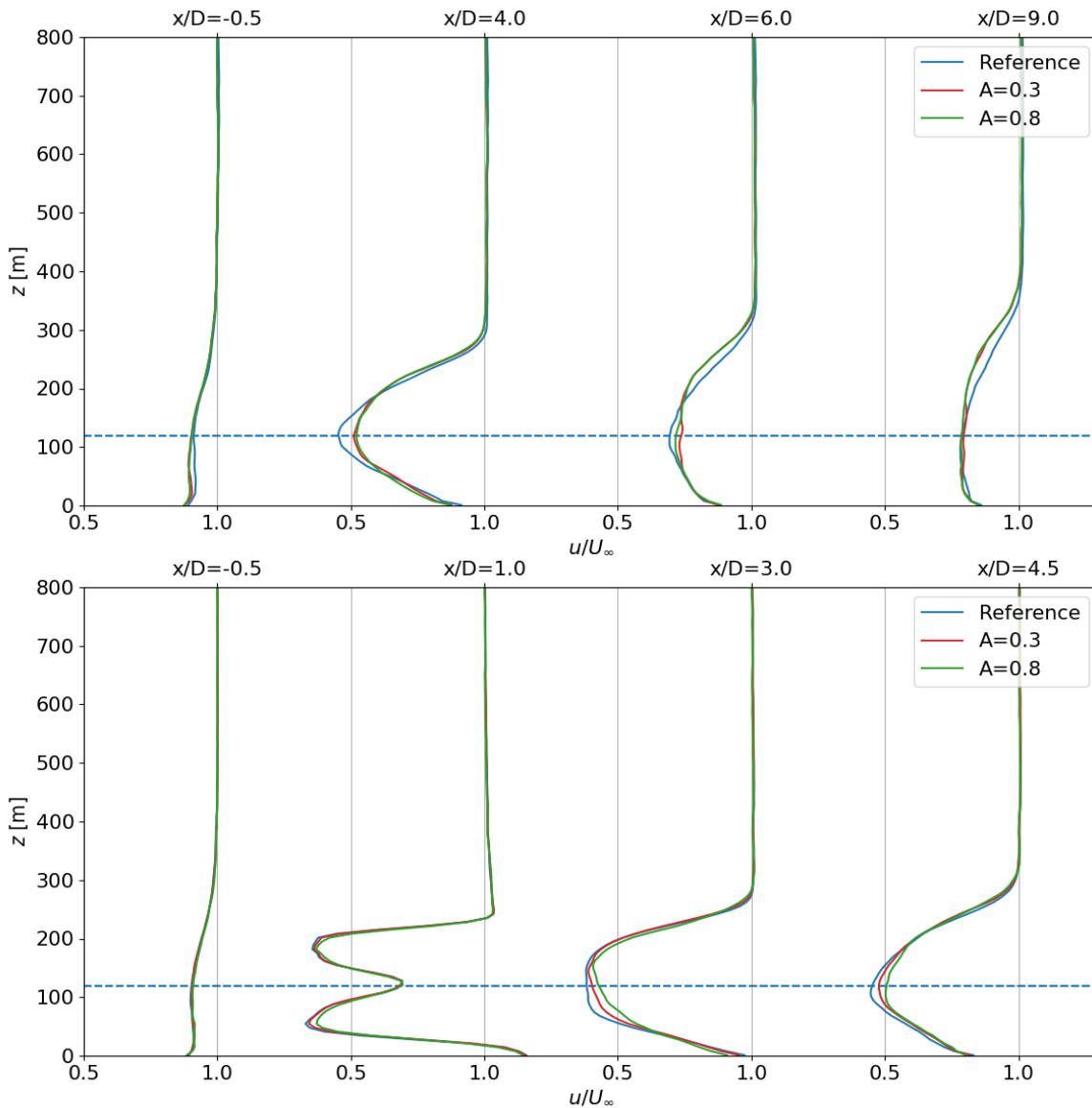


FIGURE 10 TIME AVERAGED WAKE RECOVERY DOWNSTREAM FROM THE CONTROLLED TURBINE. TOP FIGURE CORRESPONDS TO CASES 1 AND 2, BOTTOM TO CASES 3 AND 4.

5.3 POWER PRODUCTION

A direct consequence of the enhanced wake recovery observed in the previous section can be seen in Figure 11, with increased average power production of the downstream turbine when compared to the reference case. It can also be deduced that in accordance to the wake recovery

observations, the mean power increase is greatest for the 5D spacing and amplitude 0.6. However it is important to note that the 95% confidence interval error bars on the mean power overlap for WT 17, therefore the power gains are not statistically significant. Power gains for the all the turbines in the controlled rows are shown in Figure 12. It can be seen that the gain in power produced for the downstream turbines does not compensate the loss in power for the dynamically controlled turbine in cases 1 and 3, with the lower amplitude of 0.3. The highest power gain of 3% is observed with the higher amplitude of 0.6, and tighter spacing of 5D.

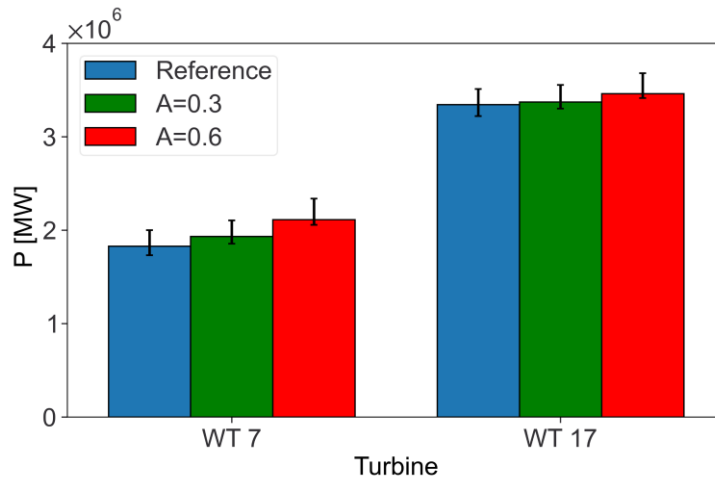


FIGURE 11 POWER PRODUCTION OF DOWNSTREAM TURBINES WT 7 AND WT17 FOR THE REFERENCE AND DYNAMICALLY CONTROLLED CASES. ERROR BARS REPRESENT 95% CONFIDENCE INTERVAL ON THE MEANS, EVALUATED USING THE BLOCK BOOTSTRAP METHOD.

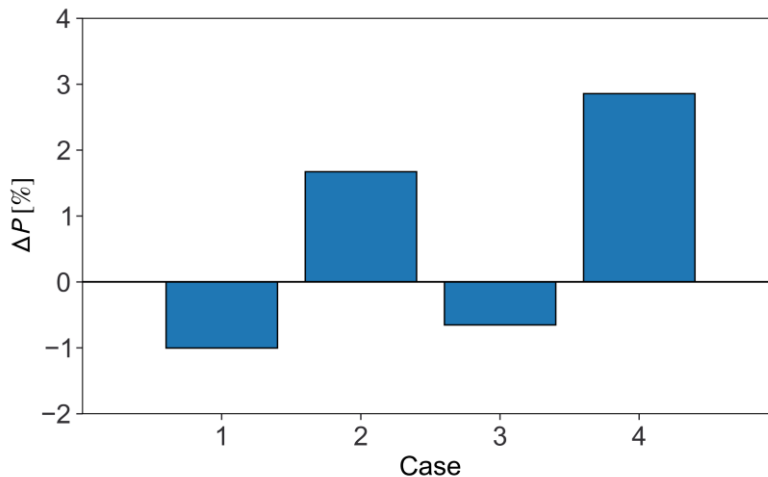


FIGURE 12 TOTAL POWER GAINS DUE TO DAIC WHEN COMPARED TO NORMAL OPERATION.

5.4 TURBINE FATIGUE

To determine the effect of dynamic induction control on the structural lifetime of the turbines, we use Damage Equivalent Loads (DELs) to compare the load histories of the turbines across the windfarm for the normal and optimal wake steering cases. DEL of each turbine is computed using the Palmgren-Miner rule and the Wöhler equation to account for accumulating fatigue damage caused to the wind turbine components by the fluctuating structural loads [12]. The loads time series are counted and binned into individual cycles using the rainflow-counting

algorithm [13]. For the wind turbine blades the components follow the Wöhler's curve with a slope coefficient equal to 10, and equal to 2 for the tower. For the dynamically controller turbine, blade root flapwise DELs are shown in Figure 13, and tower base DELs are shown in Figure 14. It can be observed that for all the cases, the windfarm experiences significant increase in damage due to fatigue, with the higher amplitude of 0.6 leading to almost a 2 times increase in fatigue in turbine components when compared to normal MPPT operation. The reason for this increase in damage can be explained by the fact that the controlled turbines are subjected to higher fatigue loads due to the constantly varying thrust forces on the rotor as a consequence of tracking a dynamically changing thrust coefficient. Fatigue along the entire turbine row is further investigated for case 4, which resulted in the highest power production. It can be observed from Figure 15 that while a few of the downstream turbines experience lower fatigue damage, it does not compensate the high fatigue experienced by the upstream dynamically controlled turbine.

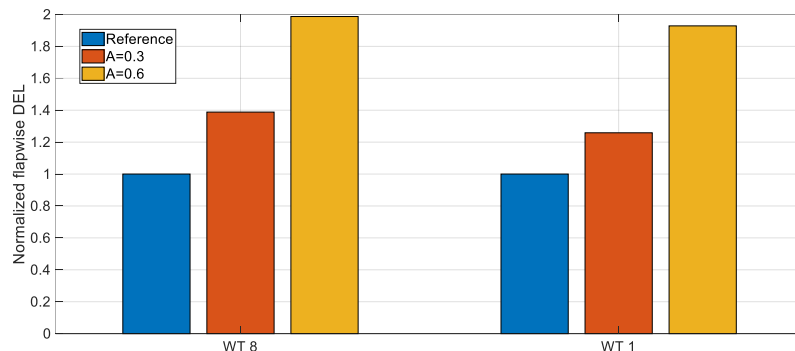


FIGURE 13 BLADE ROOT FLAPWISE DEL FOR DYNAMICALLY CONTROLLED TURBINES. DELS ARE NORMALIZED BY NORMAL OPERATION.

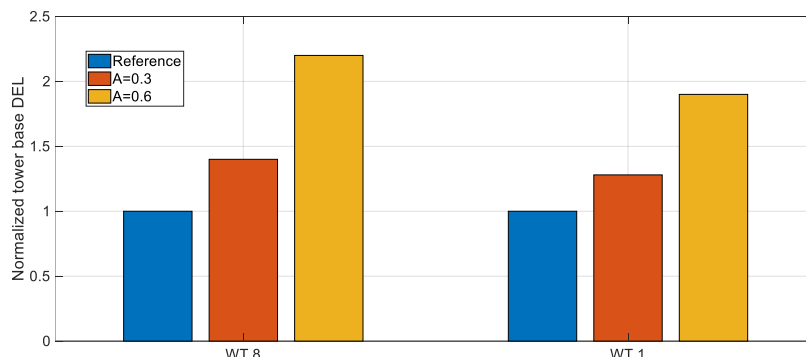


FIGURE 14 TOWER BASE DEL FOR DYNAMICALLY CONTROLLED TURBINES. DELS ARE NORMALIZED BY NORMAL OPERATION.

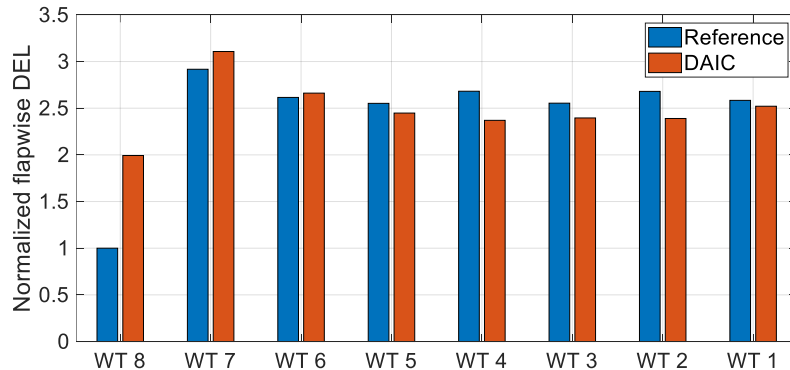


FIGURE 15 BLADE ROOT DEL FOR ALL TURBINES IN THE CONTROLLED ROW FOR CASE 4. NORMALIZATION IS DONE BY THE FIRST TURBINE UNDER NORMAL OPERATION.

6. CONCLUSIONS

In this work, a feasibility study was conducted on the Dynamical Axial Induction Control (DAIC) strategy for improving wind farm performance. By tracking a simple sinusoidal thrust coefficient signal in a virtual wind farm environment, it was observed that the control strategy lead to enhanced wake breakdown and power generation of downstream turbines, with overall gains up to 3%. The benefits however were limited to very specific modes of operation, where wind turbines were tightly spaced and a high amplitude of the thrust coefficient was used. Furthermore through the use of an aeroelastic turbine model, it was discovered that while tracking of dynamically varying thrust signals lead to increased power production in specific scenarios, the strategy always lead to a significant increase in fatigue up to 200% for the controlled turbine. Therefore, to achieve maximum benefit from the control strategy, it should only be employed for a wind farm in shorter time windows when the wind direction leads to a tightly aligned configuration, and the electricity prices justify the increase in power production at the cost of increased structural fatigue.

7. BIBLIOGRAPHY

- [1] J. P. Goit and J. Meyers, "Optimal control of energy extraction in wind-farm boundary layers," *J. Fluid Mech.*, vol. 768, pp. 5–50, 2015, doi: 10.1017/jfm.2015.70.
- [2] W. Munters and J. Meyers, "Dynamic strategies for yaw and induction control of wind farms based on large-eddy simulation and optimization," *Energies*, vol. 11, no. 1, 2018, doi: 10.3390/en11010177.
- [3] W. Munters and J. Meyers, "Towards practical dynamic induction control of wind farms: Analysis of optimally controlled wind-farm boundary layers and sinusoidal induction control of first-row turbines," *Wind Energy Sci.*, vol. 3, no. 1, pp. 409–425, 2018, doi: 10.5194/wes-3-409-2018.
- [4] A. E. Yilmaz and J. Meyers, "Optimal dynamic induction control of a pair of inline wind turbines," *Phys. Fluids*, vol. 30, no. 8, 2018, doi: 10.1063/1.5038600.
- [5] A. Vitsas and J. Meyers, "Multiscale aeroelastic simulations of large wind farms in the atmospheric boundary layer," *J. Phys. Conf. Ser.*, vol. 753, no. 8, p. 082020, Sep. 2016, doi: 10.1088/1742-6596/753/8/082020.
- [6] V. Sohoni, S. C. Gupta, and R. K. Nema, "A Critical Review on Wind Turbine Power Curve Modelling Techniques and Their Applications in Wind Based Energy Systems," *J. Energy*, vol. 2016, no. region 4, pp. 1–18, 2016, doi: 10.1155/2016/8519785.
- [7] F. Meng, W. H. Lio, and T. Barlas, "DTUWEC: An open-source DTU Wind Energy Controller with advanced industrial features," 2020, doi: 10.1088/1742-6596/1618/2/022009.
- [8] J. M. Jonkman, G. J. Hayman, B. J. Jonkman, and R. R. Damiani, "AeroDyn v15 User's Guide and Theory Manual," *Renew. Energy*, no. March, p. 46, 2015.
- [9] S. J. Anderson, J. Meyers, I. Sood, and N. Troldborg, "TotalControl D 1.04 Flow Database for reference wind farms." 2020.
- [10] D. Allaerts and J. Meyers, "Large eddy simulation of a large wind-turbine array in a conventionally neutral atmospheric boundary layer," *Phys. Fluids*, vol. 27, no. 6, 2015, doi: 10.1063/1.4922339.
- [11] W. Munters, C. Meneveau, and J. Meyers, "Turbulent Inflow Precursor Method with Time-Varying Direction for Large-Eddy Simulations and Applications to Wind Farms," *Boundary-Layer Meteorol.*, vol. 159, no. 2, pp. 305–328, 2016, doi: 10.1007/s10546-016-0127-z.
- [12] Sutherland, "Fatigue analysis of wind turbines. Technical report, Sandia National Laboratories," 1999.
- [13] D. F. Socie and S. D. Downing, "Simple Rainflow Counting Algorithms," *Int. J. Fatigue*, vol. 4, no. 1, pp. 31–40, 1982, [Online]. Available: <http://masters.donntu.org/2015/fimm/zinchencko/library/article11.pdf>.